View metadata, citation and similar papers at core.ac.uk

brought to you by CORE

provided by Portsmouth University Research Portal (Pure)

Near tip strain evolution of a growing fatigue crack

M.-L. Zhu
University of Portsmouth, UK
East China University of Science and Technology, China

Y.-W. Lu, C. Lupton, J. Tong
University of Portsmouth, UK
jie.tong@port.ac.uk

ABSTRACT. Near tip full-field strains in a growing fatigue crack have been studied *in situ* using the Digital Image Correlation (DIC) technique in a compact tension specimen of stainless steel 316L under tension-tension cyclic loading. An error analysis of displacements and strains has been carried out, and the results show that the precision of displacements and strains in the wake of the crack is worse than that in front of the crack. A method for the determination of crack tip location is proposed for the DIC analysis. Strain ratchetting is observed ahead of the growing fatigue crack tip and found to be dependent on the distance to the crack tip; whilst normal strains appear to stabilise behind the crack tip.

KEYWORDS. DIC; Crack tip; Error analysis; Fatigue crack growth; Strain ratchetting.

INTRODUCTION

Although strain-based approaches have been proposed [1, 2] to deal with fatigue crack growth since the 60s, our interest in this line of enquiry began some 10 years ago, mainly using numerical simulations [3-7], where near-tip strain ratchetting was found to be common in several materials, regardless the constitutive laws used [3-5] or the numerical simulation strategies [4-6]. We hypothesise that if the normal strain near and ahead of the crack tip continues to accumulate with fatigue cycles, the material ahead of the crack tip will eventually fail thus prompting crack growth. Although this concept has been successfully applied to rationalise fatigue crack growth in nickel-based superalloys [3], direct experimental validation was not possible until very recently, when the first experimental evidence of near-tip strain ratchetting was reported for stationary [8] and growing cracks [9] using *in situ* DIC systems.

The strain distribution near a fatigue crack tip obtained from the DIC analysis may be influenced by data processing parameters used in the DIC analysis. An accurate assessment of the near-tip strains based on the DIC technique requires the knowledge of the errors in the measured displacements and strains; hence methods may be developed in the testing and analysis to minimize the errors. Strain ratchetting behaviour has been observed for relatively straight cracks [8, 9], whilst evaluation of the strain evolution in a growing crack along a tortuous path is more challenging. Determination of the exact location of the crack tip in such a situation is another challenge, which is important to a quantitative interpretation of crack tip micro-mechanical behaviour.

In the present work, we report an error assessment of the displacements and strains measured using the DIC system; and a method to determine the locations of the instantaneous crack tip with a tortuous path. The evolution of normal strain range with fatigue cycles was tracked and the critical strain values at incipient crack growth were obtained.

EXPERIMENTAL METHODS

The material studied is stainless steel 316L, which has yield strength of 280 MPa. An average grain size was measured as approximately 17 μm. A standard compact-tension specimen was used, with a width of 60 mm, a thickness of 7 mm and a machined notch size of 12 mm. Pre-cracking was carried out under load-control using a load shedding scheme. The maximum load was decreased manually step-by-step from 10 kN to 6 kN, and the load was maintained constant at each step. The load ratio and loading frequency were 0.1 and 10 Hz, respectively, during the entire pre-cracking process. Crack growth was monitored by both the direct current potential-drop (DCPD) technique and surface replicas. The latter readings were taken as the true surface crack lengths whilst crack lengths from DCPD readings are indicative of the average crack lengths which were used to calculate the stress intensity factor *K*. The pre-cracking was terminated when the crack length reached 15 mm, after which a crack growth test was conducted for work reported in [9]. Further crack growth was allowed to remove the influence of pre-history and the original crack length in this work was 24.15 mm ($a/W \approx 0.4$).

A random speckle pattern was applied on to one of the specimen surfaces with graphite powder deposited on a white paint background. The random speckle pattern generated from the current study may be described by its grey level intensity profile, which was a bell-shaped distribution and was deemed appropriate for image correlation purposes. The imaging system (LAVISION, GMBH) consists of a CCD camera (2456 × 2058 pixels) and a Schneider Kreuznach F2.8 50mm lens with 100mm extension tubes. A region of interest, a rectangle of 1.67 × 1.4 mm with the crack tip in the centre, was selected for imaging in order to capture the near-tip strain data ahead and behind the crack tip. A resolution of 0.68 μm/pixel was achieved.

An increasing loading scheme was applied to grow the crack into a steady-state condition at a load ratio of 0.1, from P_{max} = 6 kN to 8.8 kN at a step about 10%. The loading waveform is trapezoidal with a 10 second loading/unloading and a 2 second hold at minimum and maximum loads. During the loading cycle, 23 images were collected during loading/unloading at a frequency of one image per second. Optical Microscopy (OM) was used to monitor the crack *in situ* and verify the crack tip position and the crack growth morphology.

DETERMINATION OF THE CRACK TIP

An accurate determination of the crack tip position during crack growth is important in the DIC analysis in order to capture accurately the strains near the crack tip. This is especially true when the resolution of the image is limited by the pixel size. In this work, we propose a method for locating the crack tip by a combination of information from OM and the displacement distribution from DIC analysis. Fig. 1 presents a flow chart of the method. Firstly, determine the horizontal position of the crack tip x_0 (in pixel) from the reference image collected by the DIC system and the image from the optical microscopy OM. The value x_0 may be determined from the reference image facilitated by the neighbouring speckles. Secondly, calculate the average displacement value $\overline{V_y}$ from the full data set of the displacement component in the Y direction. The values of V_y were obtained from image correlation between P_{max} and P_{min}. The value of y_0 for the crack tip may be obtained when $V_y(x_0, y_0)$ is equal to $\overline{V_y}$. The crack tip location (x_0, y_0) is thus determined. The rigid body displacement was removed prior to this operation. In the case of stationary cracks, the crack tip location thus determined is fixed when the same reference image is used for subsequent correlation of deformed images.

RESULTS AND DISCUSSION

To investigate the evolution of strain fields near the fatigue crack tips, a region of interest, centred at the crack tip, was imaged and analysed using the LaVision software. The correlation procedure was carried out from images collected *in situ* during the fatigue crack growth tests. The ranges of deformation and strain for each cycle were determined by correlating the deformed image at maximum load relative to a reference image, which was taken at minimum load at the beginning of each test. In addition, DIC analysis of several images collected under zero load was also carried out to assess the baseline errors for both displacement and strain. A subset size of 49 pixels by 49 pixels, or 33 μm × 33 μm, was chosen with a step size of 12 pixels, or 8.16 μm, in the DIC analysis.

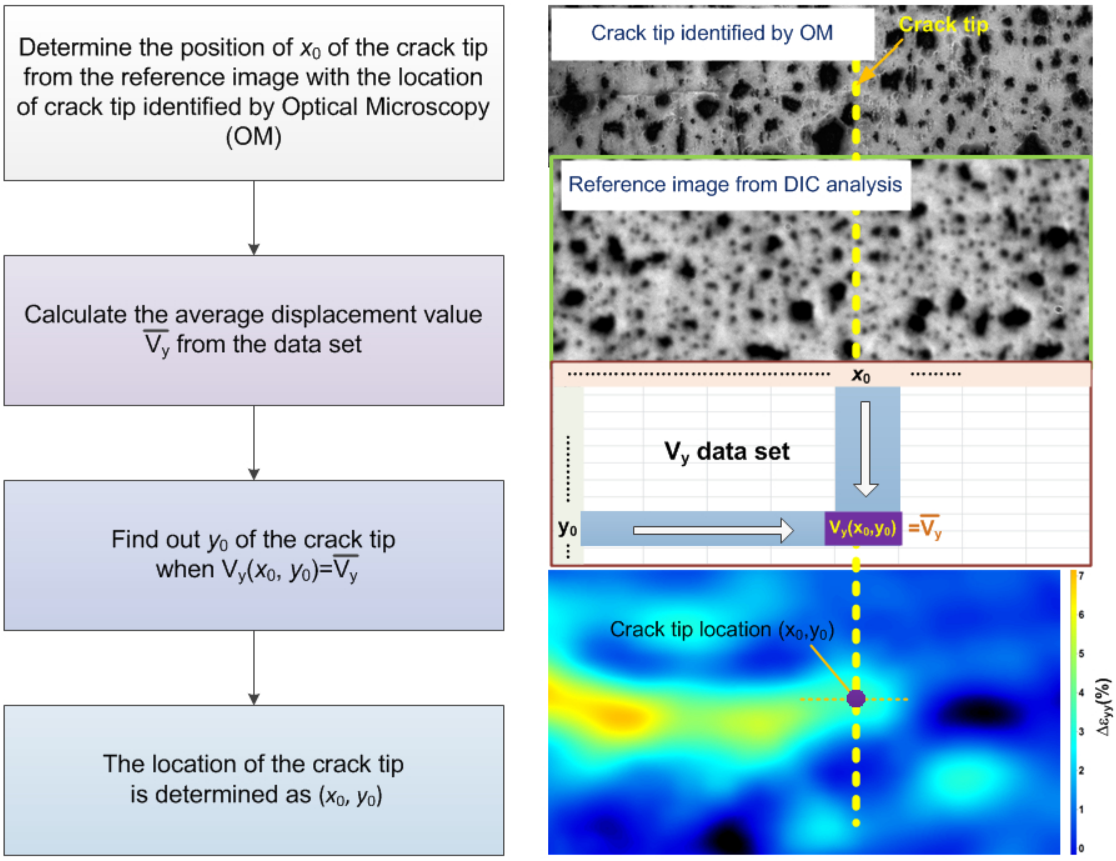

Figure 1: Schematic of the method used for locating the crack tip for DIC analysis

Error analysis

A baseline error analysis was carried out by post-processing the DIC results under zero load. The precision of displacement and strain is defined as the standard deviation of selected data points within the region of interest. The assessment was made both in front of (front) and behind (wake) the crack tip, with a square area of 0.5 × 0.5 mm chosen on both sides, as shown in Fig. 2a. Fig. 2b shows that the standard deviation of the displacements in the X and the Y directions, where the maximum error appears to be in the crack wake in the X direction, about 0.14 pixel, or 0.095 μm, although the overall errors are between 0.064 and 0.1 μm. The precision in the crack wake appears to be worse than that ahead of the crack, which is not unexpected. The strain errors are shown in Fig. 2c, where the overall error band is between 0.22% and 0.41%, again the errors in the wake are worse than those ahead of the crack tip. A possible reason may be the discontinuity due to the presence of the crack, which may have affected the speckle distribution. The precision of ε_{yy} is around 0.3%, which was deemed sufficient to give confidence in the measurement of near-tip strains in this work.

Strain evolution of a growing fatigue crack

The near-tip strains were collected during the fatigue crack growth test at a maximum cyclic load of 8.8 kN, R=0.1 and ΔK=33.5 MPa·m$^{1/2}$. Fig. 3 shows the crack growth morphology post testing. The crack deflected slowly at first, then followed a tortuous crack path, with a crack growth of about 106 μm during the last 200 cycles. This last stage of crack growth was analysed and the normal strain evolution with the number of cycles was tracked.

Fig. 4 shows the range of normal strain $\Delta\varepsilon_{yy}$ distribution in the region of interest at the 200th cycle. Selected points were used for tracking the strain evolution with the number of cycles. The tracking points were selected on the same plane, with varied distances to the initial crack tip. Points 1, 3, 5 and 7 were chosen on the crack path, and the strain values at these points were assessed with respect to the incipient crack tip location during the crack growth process. The distance to the initial crack tip at Points 3, 6 and 8 is double, 4 times and 6 times of the grain size, respectively. The strain values at the selected points were averaged over a square domain of 14 × 14 pixels (9.52 × 9.52 μm), centred at each tracking point. This is illustrated in Fig. 4, where the normal strain value at Point 1 is obtained by averaging the strain data from the square.

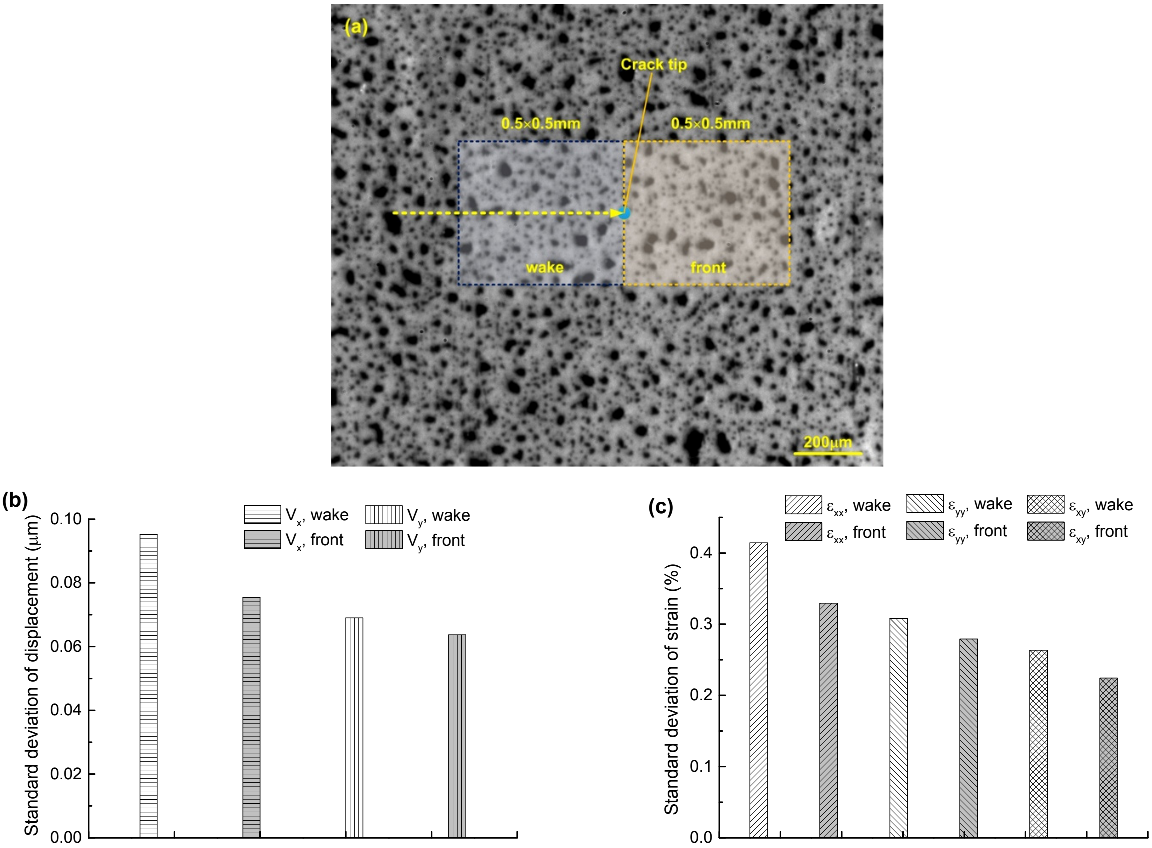

Figure 2: Error analysis of displacements and strains for both ahead of (front) and behind (wake) the crack tip under zero load: (a) An image of the region of interest (1mm×0.5mm) near the crack tip; (b) standard deviation of the displacement components and (c) standard deviation of the strain components.

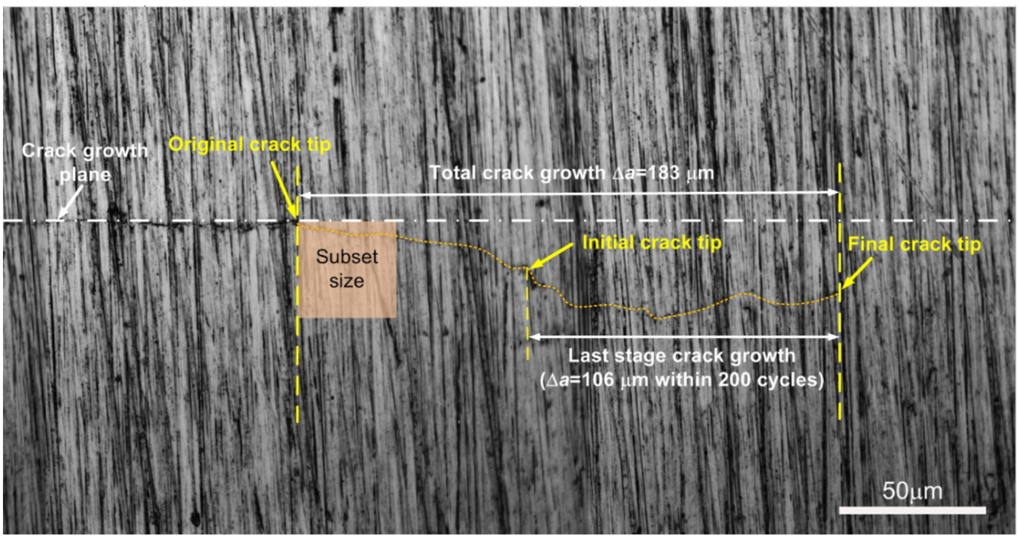

Figure 3: A fatigue crack path with the initial and final crack tips indicated. The last stage of the crack growth was considered in the strain analysis using DIC.

The evolution of strain range with the number of cycles at the selected tracking points is shown in Fig. 5. The normal strain range generally increases with the increase of fatigue cycles, clearly indicating strain ratchetting. Similar strain evolution patterns may be observed at Points 1-3; also at Points 4-8. The reduced strains measured during early stages of crack growth may be due to the deflection of the crack growth path (Fig. 3 and 4), thereafter the strains continue to increase. Although no attempt was made to obtain the local normal strains along the tortuous crack path, the normal strains tracked at the selected points appear to behave similarly, indicating strain ratchetting is consistently observed near the crack tip. Assuming the fatigue crack growth is steady state, the transient crack tip location is estimated to be at A, B, C and D for Points 1, 3, 5 and 7, respectively. The normal strain range at these positions appears to be from around 8% (A) to 9.4% (D). A strain range of about 8% might be indicative of a critical value above which steady state fatigue crack growth occurred, consistent with our previous results [9]. It is of interest to note that the strain values from Points 1-6 at the 200th cycle are similar, suggesting that the strains in the wake of the crack tend to stabilize.

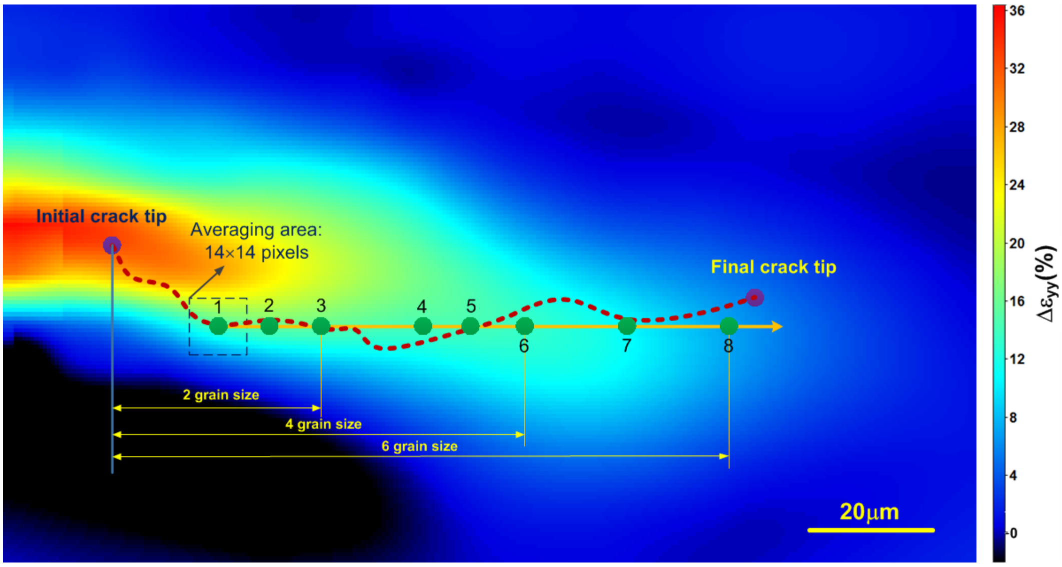

Figure 4: The normal strain range distribution and the tracking points for strain measurement at N=200. Points 3, 6, 8 were chosen to be 2, 4 and 6 times of the average grain size; Points 1, 3, 5, 7 were chosen on the crack path.

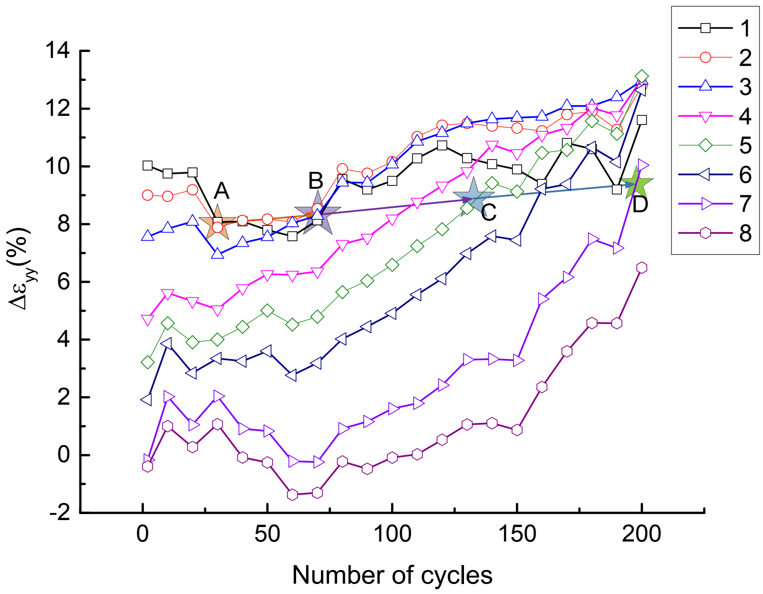

Figure 5: The evolution of the normal strain ranges at the selected tracking points as a function of number of cycles. The stars indicate the strains at which incipient crack growth occurred.

CONCLUSIONS

The evolution of normal strain range with cycle has been captured *in situ* during the fatigue crack growth experiments using the DIC technique in a compact tension specimen of stainless steel 316L. Generally, the normal strain range measured is between 4% and 13% near the crack tip, hence the relative error in the measurements is no more than 7.5%. A method to determine the crack tip location is proposed for a crack with a tortuous crack path. Strain ratchetting is observed in the near-tip field ahead of the crack tip, whilst normal strains behind the crack tip appear to be more stable.

ACKNOWLEDGEMENTS

MLZ is supported by a Visiting Scholarship from China Scholarship Council.

REFERENCES

[1] McClintock, F.A., On the plasticity of the growth of fatigue cracks, John Wiley & Sons Inc., New York, (1963).
[2] Haigh, J.R., Skelton, R.P., A strain intensity approach to high temperature fatigue crack growth and failure, Mater. Sci. Eng., 36 (1978) 133-137.
[3] Zhao, L.G., Tong, J., Byrne, J., The evolution of the stress – strain fields near a fatigue crack tip and plasticity-induced crack closure revisited, Fatigue. Fract. Eng. Mater. Struct., 27 (2004) 19-29.
[4] Zhao, L., Tong, J., A viscoplastic study of crack-tip deformation and crack growth in a nickel-based superalloy at elevated temperature, J. Mech. Phys. Solids., 56 (2008) 3363-3378.
[5] Lin, B., Zhao, L.G., Tong, J., A crystal plasticity study of cyclic constitutive behaviour, crack-tip deformation and crack-growth path for a polycrystalline nickel-based superalloy, Eng. Fract. Mech., 78 (2011) 2174-2192.
[6] Huang, M., Tong, J., Li, Z., A study of fatigue crack tip characteristics using discrete dislocation dynamics, Int. J. Plast., 54 (2014) 229-246.
[7] Tong, J., Zhao, L.G., Lin, B., Ratchetting strain as a driving force for fatigue crack growth, Int. J. Fatigue., 46 (2013) 49-57.
[8] Tong, J., Lin, B., Lu, Y.W., Madi, K., Tai, Y.H., Yates, J.R., Doquet, V., Near-tip strain evolution under cyclic loading: In situ experimental observation and numerical modelling, Int. J. Fatigue., 71 (2015) 45-52.
[9] Lu Y.-W., Lupton, C., Zhu, M.-L., Tong, J., In situ experimental characterization of near-tip strain evolution of fatigue cracks, Exp. Mech., (2015) In press.